Turkish Journal of Electrical Engineering & Computer Sciences

http://journals.tubitak.gov.tr/elektrik/

Research Article

Turk J Elec Eng & Comp Sci
(2017) 25: 3764 – 3775

doi:10.3906/elk-1606-180

Fault location determination for transmission lines with different series-compensation levels using transient frequencies

Düzgün AKMAZ[1], Mehmet Salih MAMİŞ[2,*], Müslüm ARKAN[2], Mehmet Emin TAĞLUK[2]
[1]Department of Electrical and Electronics Engineering, Faculty of Engineering, Munzur University, Tunceli, Turkey
[2]Department of Electrical and Electronics Engineering, Faculty of Engineering, İnönü University, Malatya, Turkey

Received: 13.06.2016 • **Accepted/Published Online:** 18.05.2017 • **Final Version:** 05.10.2017

Abstract: In this paper, based on the theory of traveling waves, the fault distances on long transmission lines with various series-compensation levels are determined using transient current and voltage frequencies. Transmission lines with series compensation are modeled using Alternative Transients Program software with frequency-dependent effects on the line included in the simulation. The transient current and voltage signals are obtained from the model. A fast Fourier transform is used for frequency-domain conversion and fault location is estimated from the frequencies of fault-generated harmonics in the transient spectrum. The algorithm is implemented in MATLAB. To investigate the effect of compensation on accuracy, the results are obtained for different series-compensation levels. The undesirable source-inductance effect is removed and estimation accuracy is further improved using a waveform-relaxation method. The method is found to be successful in determining fault location on series-compensated transmission lines. The effects of the compensation level, fault resistance, and phase angle are investigated.

Key words: Fault location estimation, traveling waves, series compensation, transmission lines, transients

1. Introduction

Series compensation is a practical and economical solution in reducing reactance for long transmission lines, thereby improving their voltage profile and increasing line-transfer capability; this results in less reactive power consumption and transmission-line loss [1–4]. Although series compensation is provided by capacitors, a protective circuit is required in the case of failure, when the voltage on the capacitor may exceed its normal value, damaging it. Metal oxide varistors (MOVs) and air gaps are used as typical protective circuits [5–8]. However, the nonlinear behaviors of MOVs may affect accuracy [4].

The techniques for fault location can be classified as phasor-measurement-unit (PMU)-based algorithms [9,10], time-domain-line-model-based techniques with distributed parameters [11,12], and traveling wave-based methods [13,14]. PMU-based algorithms utilize two different approaches for estimation of the fault distance, namely one-end [9] or two-end measurements [10].

Some papers have used the distributed time-domain linear model, which has good accuracy for estimating fault location, regardless of the fault type, inception angle, or impedance of the fault [11,12]. However, current and voltage samples must be synchronously taken from the two ends of the line, which is sometimes difficult.

Traveling wave-based algorithms that employ wavelet transforms are another class of methods for estimating fault location on series-compensated lines [13,14]. They are applicable to any network configurations

*Correspondence: mehmet.mamis@inonu.edu.tr

and neither the impedance nor the inception angle in any type of fault influences the accuracy. However, a high sampling rate is required for analysis [13,14].

A transient signal spectrum, in conjunction with the traveling wave theory, can also be used for fault-distance determination [15,16]. This method has been previously tested for uncompensated [15,16] and series-compensated transmission lines [17,18]. In [17], a transmission line with series compensation is considered and the location of a line-to-ground fault was estimated; however, the protection circuit was not considered in the simulations. In [18], all types of faults were considered on a long transmission line with a series-compensation model comprising a capacitor, as well as a protection circuit comprising an MOV and an air gap with an RL damping circuit. However, different series-compensation levels have yet to be tested. In this study, the method is extended to estimating fault location on long transmission lines with different series-compensation levels for all fault conditions and types. Alternative Transients Program (ATP) software [19] is used to simulate a series-compensation line model to obtain transient voltage and current samples, and the developed algorithms are implemented in MATLAB. The results obtained show that the method is successful at estimating the locations of the faults of transmission lines with series compensation. In addition, the method is not influenced by the compensation level, the phase angle at the instant of the fault, or the resistance of the fault point.

This paper is organized as follows: after the introduction, the series-compensation design on long transmission lines is presented in Section 2. In Section 3, the theory of traveling wave-based fault-estimation method is given. In Section 4, the simulation model and the application results are presented and the effects of fault resistance, phase angle, source inductance, and compensation level are investigated.

2. Series-compensation model

Fixed or controllable capacitors are used for the compensation of transmission lines. Each technique has different advantages. Control over the line's power flow can be better achieved by electronically controlled series compensation [3]. However, this may influence the load current, as well as certain system parameters such as line impedance [3]. Therefore, in this study, a fixed-capacitor series-compensation model, which is preferred in common usage, is considered in the simulations.

The fixed-capacitor model installed on a long transmission line is composed of three main units. These are the capacitors, the MOV, and the air gap with RL damping, as depicted in Figure 1. The functions of these three units are explained next.

2.1. Capacitor unit

Series compensation is performed by placing capacitors at the midpoint or at both ends of a line to reduce inductive-reactance and to increase loading capacity. This ensures a much more stable system with reduced system losses. The influence of series compensation on a transmission line depends on the compensation degree (k), which is determined as:

$$k = X_C/X_L \tag{1}$$

Here, X_C represents the capacitive-reactance value of the capacitor, and X_L represents the inductive reactance of the line. Optimal values of the series-compensation level range from 30% to 70% depending on the application [1]. In the case of failure, the voltage on the capacitor may sometimes exceed its rating voltage. In this case, the capacitor needs protection and therefore control circuits are intended to prevent the capacitor from being damaged in this situation. Commonly proposed protection circuits include MOVs and air gaps with RL damping [5–8].

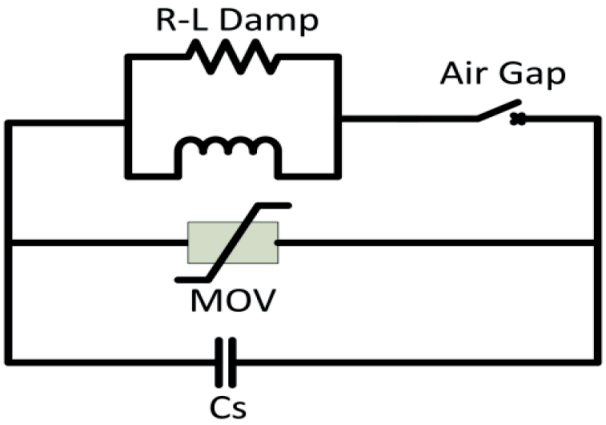

Figure 1. Model for series compensation. For 50% compensation: Cs = 31.4 μF, L = 0.23 mH with 5 Ω resistor in series, R = 200 Ω, and 110 kV, 9 MJ MOV. For 70% compensation: Cs = 22.4 μF, L = 0.23 mH with 5 Ω resistor in series, R = 200 Ω, and 150 kV, 9 MJ MOV.

2.2. MOV unit

MOVs are circuit elements that offer capacitors protection against high voltages [1,3–8]. In the series-compensation model, the line current is divided into two components: the capacitor and the MOV currents. The current does not pass through an MOV under normal conditions but, during a failure, such a current can occur as a consequence of the high voltage level on the capacitor [4]. The VI characteristic of the MOV is nonlinear and can be described using the following equation:

$$I = p\left(\frac{V}{V_{ref}}\right)^{q} \tag{2}$$

where V_{ref} and p are defined as the reference quantities of MOV, and exponent q is typically of the order of 20–30 [4]. The reference voltage value of the MOV can be determined with the following equation [8]:

$$v_{ref} = 2.5\cdot \text{ Current } \cdot X_C \cdot \sqrt{2} \tag{3}$$

In this equation, the protection level required to protect the capacitors is typically 2.5 times the nominal system voltage.

2.3. Air gap with RL damping unit

After compensation, the energy value of the MOV can sometimes be at a dangerous level, so an air gap is employed to protect the MOVs and capacitors [7,8]. The air gap sparkles over at a particular voltage level, and the RL damping system, which consists of a parallel connected inductor and resistor, serves to limit the current [7,8].

3. Fault-distance estimation using the traveling wave theory

Although the theory of traveling waves has already been presented in [20], its outlines are repeated here for convenience. To calculate the voltage and current phasors $\boldsymbol{V}$ and $\boldsymbol{I}$ at any point on the line, the following equations can be used [20]:

$$\mathbf{V} = C_1 e^{\gamma x} + C_2 e^{-\gamma x}, \tag{4}$$

$$\mathbf{I} = \frac{1}{z_0}C_1 e^{\gamma x} - \frac{1}{z_0}C_2 e^{-\gamma x}, \tag{5}$$

where $\gamma = \sqrt{zy}$ is the propagation constant, $z_o = \sqrt{z/y}$ is the surge impedance of the line, z is the series impedance, and y is the shunt admittance per unit length.

The constants C_1 and C_2 are evaluated based on the boundary conditions of the transmission line. The propagation constant is written as $\gamma = \alpha + j\beta$, where α is the attenuation constant measured in nepers per unit length and β is the phase constant in radians per unit length. If β is the phase shift in radians per km, the wavelength λ in km is:

$$\lambda = \frac{2\pi}{\beta}. \tag{6}$$

The propagation velocity is then determined as $v = \lambda f$, which is also

$$v \approx \frac{1}{\sqrt{lc}} \tag{7}$$

in terms of the line parameters inductance, l, and capacitance, c. Let τ_f be the surge-travel time from the point of the fault to the point of measuring, which is determined as:

$$\tau_f = \frac{x}{v}. \tag{8}$$

Here, x is the fault distance. If the speed of the wave and the transient frequency $f_i d$ is known, the following equation can be used to determine the fault distance [15–18]:

$$x = v\tau_f = \frac{iv}{2f_i} \tag{9}$$

4. Simulation model

In this study, a 50-Hz, 380-kV overhead transmission line of length 600 km is simulated. The tower configuration of the transmission system is illustrated in Figure 2 and the physical parameters for the lines are given in [16]. The simulation model for the transmission system without series compensation in ATPDraw is shown in Figure 3. In Figure 4, an ATPDraw model of the series-compensated transmission system is shown.

In the simulation, the series-compensation model is localized at the midpoint. Therefore, depending on whether the fault is located in the first half (before the midpoint) or the second half (after the midpoint) of the line, two different network configurations, each having three line sections, are considered for fault analysis. For a fault located before the midpoint of the line, the compensation-circuit model is installed after the 2nd line model, as shown in Figure 4a. The 3rd line maintains a constant length of 300 km. For a fault located after the midpoint of the line, the compensation-circuit model is installed after the 1st line, as shown in Figure 4b.

As fault-generated transient frequencies are always greater than the power frequency, a frequency-dependent line model should be used. Therefore, Marti's line model was chosen for this study [21]. This line model is currently used in most transient-analysis programs and has been shown to be accurate and efficient in most simulation cases [22].

After obtaining the current and voltage waveforms from the simulations, a modal transformation is applied. Positive-sequence current and voltage data are employed for fault-distance determination since the

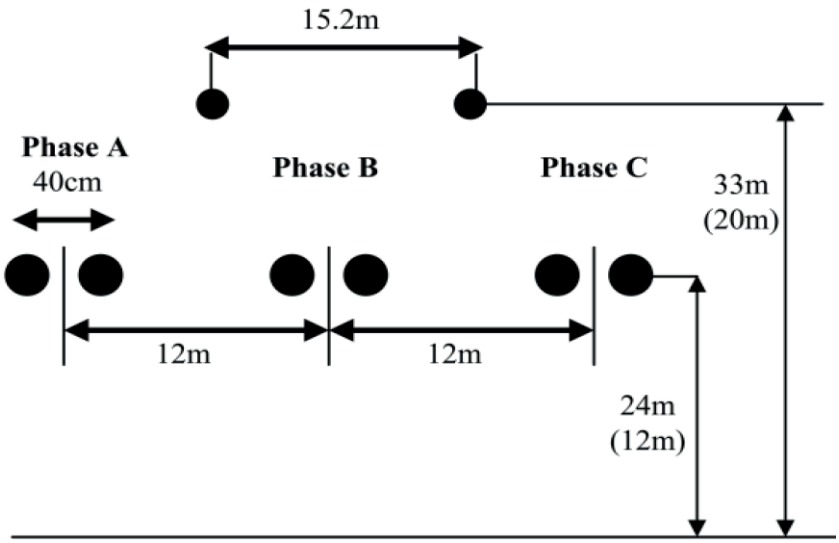

Figure 2. Tower configuration for the 380-kV test system.

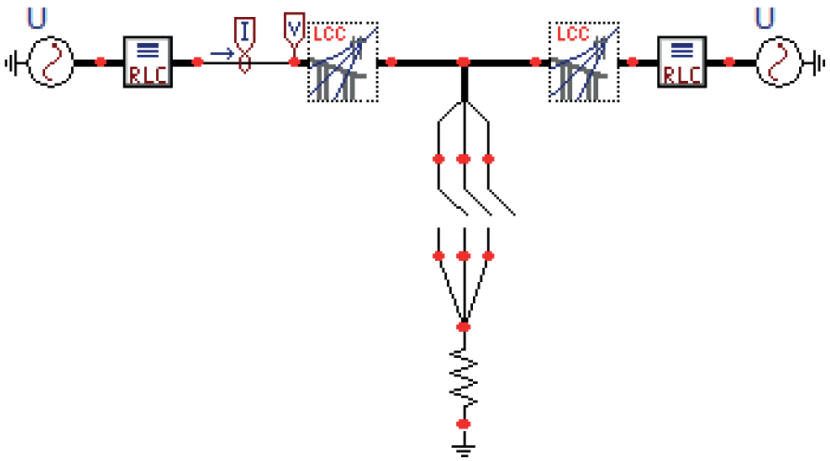

Figure 3. Two-terminal power network without a series compensation.

positive-sequence inductance of the overhead lines is independent of frequency. The voltage and current quantities are transformed to the modal ones by:

$$\mathbf{I}_m = \mathbf{T}^{-1} I_p \text{ and } \mathbf{V}_m = \mathbf{T}^{-1} V_p, \tag{10}$$

where the subscripts p and m are used to define the phase and modal quantities, respectively. For a three-phase line with transposed conductors, the transformation matrix and its inverse are:

$$T = \begin{bmatrix} 1 & 1 & 0 \\ 1 & 0 & 1 \\ 1 & -1 & -1 \end{bmatrix} \text{ and } T^{-1} = \frac{1}{3} \begin{bmatrix} 1 & 1 & 1 \\ 2 & -1 & -1 \\ -1 & 2 & -1 \end{bmatrix}. \tag{11}$$

A fast Fourier transform (FFT) is used for time-to-frequency conversion of the modal current and voltages. The obtained spectrum provides fault-location data.

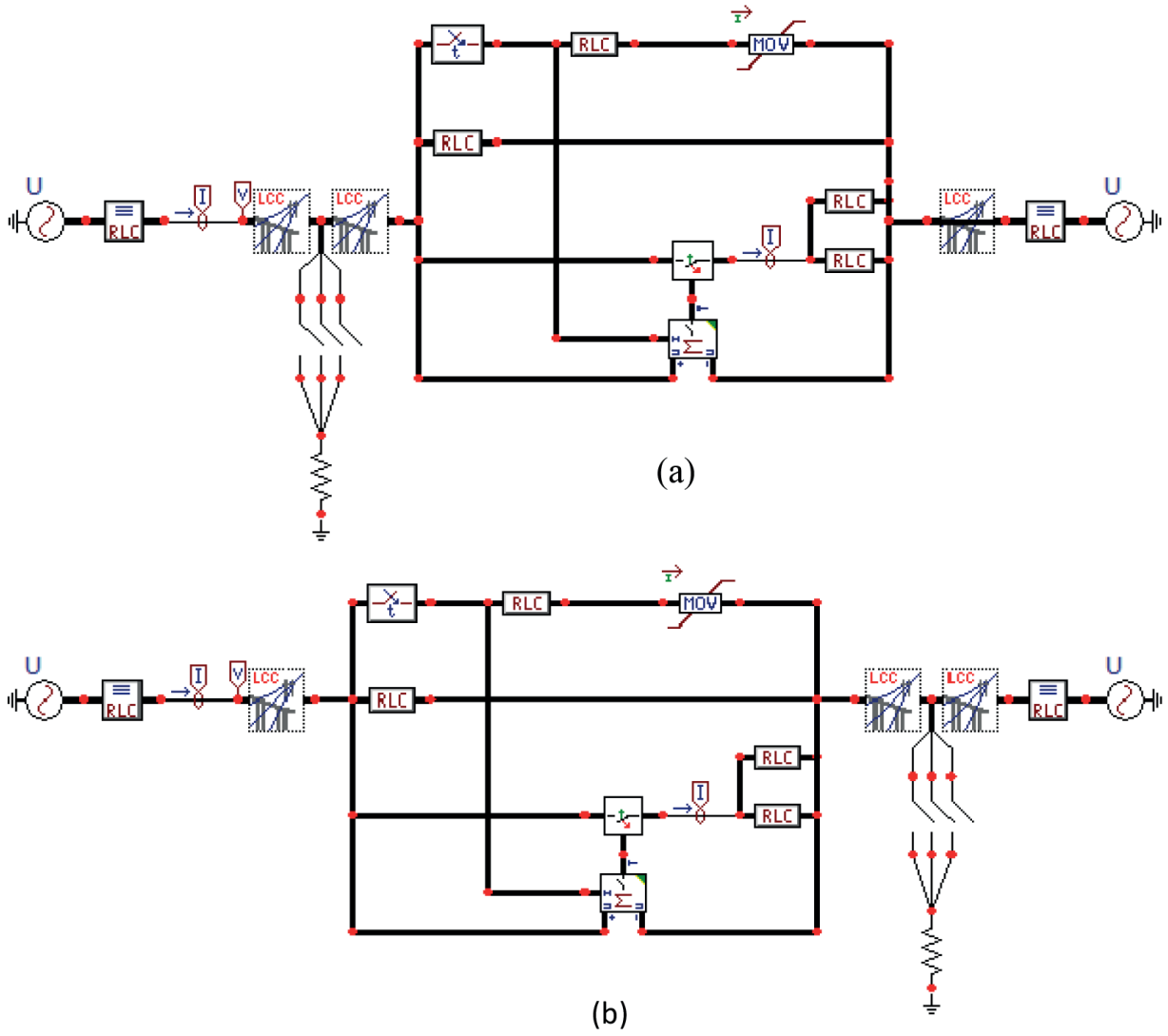

Figure 4. ATPDraw model of a long, series-compensated transmission line: a) fault before midpoint, b) fault after midpoint.

5. Simulation results

In the test network, the source resistance and inductance are selected to be 0.1 Ω and 1 mH, respectively. The calculated line inductance is l = 1.075 mH/km and the capacitance of the transmission line is c = 10.805 nF/km for the positive sequence [16]. Surge velocity, as calculated from these values, is $v = (1/lc)^{1/2} = 294.32 \times 10^3$ km/s. The line inductance is needed to determine the value of the compensation capacitor. The total inductive reactance of the transmission line is 202.53 Ω. When 50% compensation is applied, the capacitive reactance is 101.2 Ω, and the required capacitance for series compensation is 31.4 μF at the assumed power frequency. In the case of 70% compensation, the capacitive reactance is 141.771 Ω and the capacitance is 22.4 μF.

In Eq. (3), the line current and reference voltage for the MOV are chosen as 300 A and 110 kV for 50% series compensation, and the line current and reference voltage for the MOV are chosen as 300 A and 150 kV

for 70% series compensation, respectively. The energy absorption rate of the MOV is taken as 9 MJ. A 0.01-Ω resistor is connected in series to the MOV. The RL damping unit consists of a 0.23-mH inductor and a 200-Ω resistor connected in parallel, as well a 5-Ω resistor connected in series with the inductor.

A Hanning window and zero padding are used to reduce FFT leakage and to increase FFT resolution, respectively, for positive-sequence transient signals. The FFTs of positive-sequence transient currents and voltages are then obtained in MATLAB. In accordance with Eq. (9), even if a fault occurs at a remote end of the line, the frequency of the first harmonic component is 244 Hz. For this reason, frequencies equal to or greater than this value are considered on the frequency spectrum of the transient signals. When the frequency of the traveling waves is 244 Hz, the total inductive reactance of the transmission line is 988.3 Ω. For series compensations of 50% and 70%, the reactance of the series capacitance is reduced to 21.05 Ω and 29.13 Ω, respectively, at this frequency. These values are much smaller than the series impedance of the transmission line; hence, the effect of series capacitance upon the determination of fault distance becomes negligible.

In Figure 5, the spectrums of positive-sequence transient voltage and current signals of uncompensated line for symmetrical fault (LLL) and unsymmetrical faults (line to ground (LG), line-to-line (LL), double line-to-ground fault (LLG)) at 250 km at $t = 0$ are presented. In Figure 6, the spectrums of positive-sequence transient voltage and current signals of the line with 70% compensation for symmetrical fault (LLL) and unsymmetrical faults (LG, LL, and LLG) at 250 km at $t = 0$ are presented.

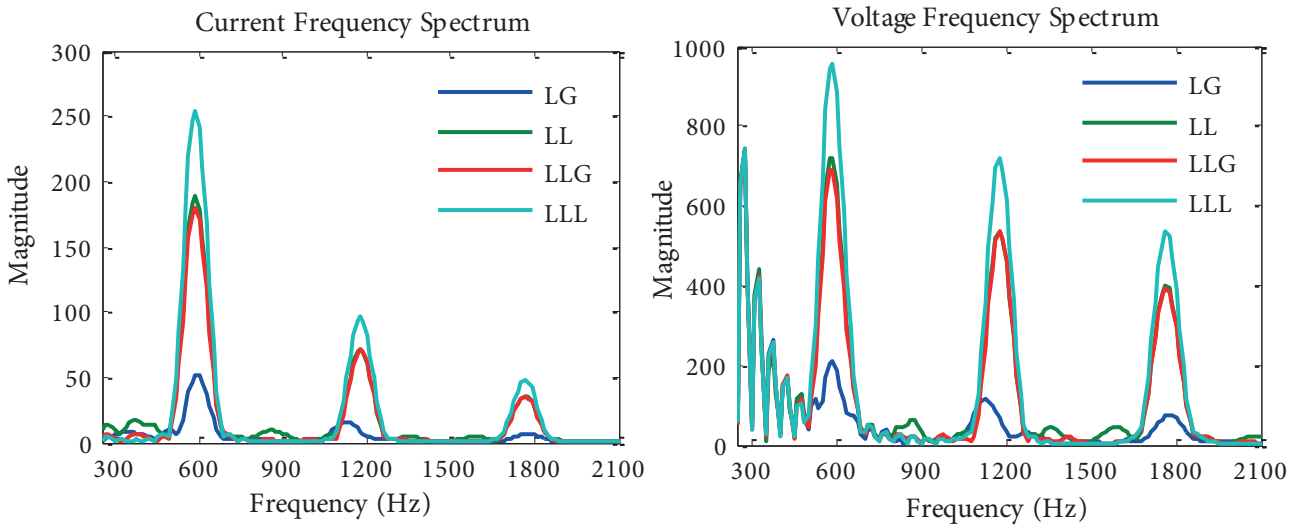

Figure 5. Spectrum of positive-sequence transient current and voltage for LG, LL, LLG, and LLL faults at 250 km on a long transmission line without series compensation.

For the uncompensated line, the measured first transient frequency in each spectrum is 587.5 Hz, which corresponds to $x = \frac{v}{2f_1} = \frac{293.42x10^3}{2x587.5} = 249.71\,km$, and the error is 0.04% in fault distance. The percentage error is determined as:

$$Percentage\,error = \frac{|Actual\,fault\,distance - Estimated\,fault\,distance|}{Total\,line\,length} \times 100 \tag{12}$$

In the case of the LL, LLG, and LLL faults, transient frequencies are very definite, as seen in Figures 5 and 6. However, in the case of the LG fault, the transient frequencies are sometimes difficult to identify. Nevertheless, fault distance can still be determined.

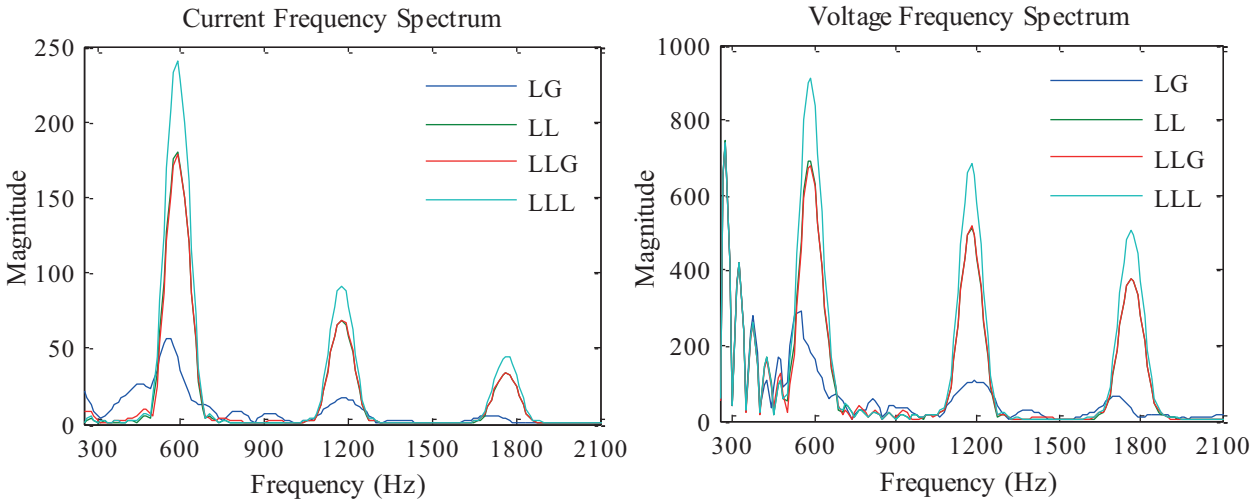

Figure 6. Spectrum of positive-sequence transient current and voltage for LG, LL, LLG, and LLL faults at 250 km on the long transmission line with 70% series compensation.

The estimated values for fault location in the case of the LG fault at several different locations and series-compensation levels are presented in Table 1. As transient frequencies are much higher than the power frequency and because the impedance of the compensation capacitor decreases as frequency increases, the effect of series compensation is very limited. For example, for a fault at 500 km, the first transient frequency is 300 Hz and the impedance of the series capacitor reduces 6 times at this frequency compared to its impedance at the power frequency. As fault distance decreases, the frequencies of the transient harmonics and the impedances of the series capacitors respectively increase and decrease accordingly.

Table 1. Estimated fault distance and accuracy for LG faults at several distances and compensation levels.

Actual fault distance (km)	Without series compensation		With 50% series compensation		With 70% series compensation	
	Estimated fault distance (km)	Percentage error	Estimated fault distance (km)	Percentage error	Estimated fault distance (km)	Percentage error
50	53.1	0.51	54	0.66	54	0.66
100	105.69	0.94	104.79	0.79	105.69	0.94
200	213.39	2.23	213.39	2.23	213.39	2.23
250	249.71	0.04	266.74	2.79	266.74	2.79
300 (after compensator)	317.21	2.87	317.21	2.87	317.21	2.87
300 (after compensator)	317.21	2.87	317.21	2.87	317.21	2.87
350	366.77	2.79	391.22	6.83	391.22	6.83
400	404.71	0.78	419.17	3.19	419.17	3.19
500	558.89	9.81	533.49	5.58	533.49	5.58

The estimated distances for other types of faults (LL, LLG, and LLL) are found to be the same, and the tabulated results for different series-compensation levels are presented in Table 2. When the results are

examined, it can be seen that the percentage error is high for the LG fault. It also is noticeable that the percentage error increases along with distance for almost all types of faults. Considering this, it can be determined that the error in fault distance can be reduced by a two-end measurement.

Table 2. Estimated fault distance and accuracy for LL, LLG, and LLL faults at several locations and compensation levels.

Actual fault distance (km)	Without series compensation		With 50% series compensation		With 70% series compensation	
	Estimated fault distance (km)	Percentage error	Estimated fault distance (km)	Percentage error	Estimated fault distance (km)	Percentage error
50	50.58	0.09	50.58	0.09	50.58	0.09
100	100.28	0.04	100.28	0.04	100.28	0.04
200	198.92	0.18	198.92	0.18	198.92	0.18
250	249.71	0.04	249.71	0.04	249.71	0.04
300 (before compensator)	300.94	0.16	300.94	0.16	300.94	0.16
300 (before compensator)	300.94	0.16	300.94	0.16	300.94	0.16
350	345.2	0.80	345.2	0.80	345.2	0.8
400	404.71	0.78	404.71	0.78	391.22	1.46
500	489.03	1.82	510.29	1.71	489.03	1.82

In Tables 3 and 4, the effect of fault resistance and phase angle on location is presented by comparing the results obtained for different compensation levels. As can be seen from these tables, the method is not affected by fault resistance, phase angle, or series-compensation level.

Table 3. Estimated fault distance and accuracy for LLL fault at the midpoint for several fault resistance values and compensation levels.

Fault resistance (Ω)	Without compensation and with 50% and 70% series compensation	
	Estimated fault distance (km)	Percentage error
0.1	300.94	0.16
5	300.94	0.16
10	300.94	0.16
50	300.94	0.16

The effects of source inductance on fault location for a three-phase fault on transmission lines with different series-compensation levels are presented in Table 5. When the data in this table are examined, it is noticeable that the source impedance has a negative effect on the accuracy of estimated fault location. This is due to the influence of lumped inductance on wave speed. However, it has been shown that the fault distance can be determined within a reasonable error by modifying the distributed line inductance step-by-step through the inclusion of delay effects that occur due to lumped source inductance [16,18]. This procedure is known as waveform relaxation and is described here for convenience:

Table 4. Estimated fault distance and accuracy for LLL fault at the midpoint for several phase-angle values and compensation levels.

Phase angle (degree)	Without compensation and with 50% and 70% series compensation	
	Estimated fault distance (km)	Percentage error
0	300.94	0.16
90	300.94	0.16
120	300.94	0.16
150	300.94	0.16

Table 5. Estimated fault distance and accuracy before and after improvement procedures for LLL fault at the midpoint for several source inductances and compensation levels.

Source inductance (mH)	Estimated fault distance before improvement		Estimated fault distance after improvement	
	Estimated fault distance (km)	Percentage error	Estimated fault distance (km)	Percentage error
0.1	300.9	0.16	300.6	0.10
1	300.9	0.16	299.8	0.04
10	308.9	1.47	299.7	0.05
50	345.2	7.53	302.3	0.38

Step 1: Set $i = 1$ and x_i = total line length

Step 2: Calculate modified line inductance, $l_i = l + \frac{2L_s}{x_i}$

Step 3: Calculate modified propagation velocity, $v = 1/\sqrt{l_i c}$

Step 4: Calculate corrected fault distance, $x_{i+1} = v\tau$

Step 5: If $|x_{i+1} - x_i| \leq E_{\max}$ or $i = N$ stop; otherwise, increment $x_{i+1} = x_i$ and $i = i + 1$ and go to Step 2

Here, N is the maximum number of loops allowed. The estimated fault location x_i is determined using the fault-location expression presented in Step 1. The inductance of the transmission line is modified in Step 2. Wave velocity is calculated accordingly using the new inductance value of the transmission line in Step 3. The corrected fault distance is determined in Step 4 and finally the fault-location error is estimated using the subsequent results in Step 5. If the error is greater than the specified value, the algorithm will be repeated. This cycle continues until the algorithm achieves a reasonable accuracy. Tests indicate that even two loops are sufficient for reasonable accuracy.

Estimation values for several source inductances before and after improvement of the procedure are presented in Table 5. The largest error is 7.53%, which reduces to 0.38% after improvement. Using this procedure, good enhancements can be achieved for other types of faults.

6. Conclusion

Short-circuit faults may lead to considerable economic losses in power systems. Therefore, the location of a fault needs to be specified with high accuracy as soon as possible. In this study, fault distance was determined for compensated transmission lines with different series-compensation levels using a traveling wave-based method. Fault distance was detected by processing fault-generated transient voltage and current waveforms. FFT was

used to transform the time-domain signal into the frequency domain. Frequencies corresponding to peak points in the spectrum were specified as frequencies of the fault transient. The method was tested for long transmission lines for different fault-inception angles, fault resistances, fault locations, and fault types. The simulation results showed that the proposed method was successful in determining the locations of four different short-circuit faults on long transmission lines with different series-compensation levels. It was also observed that this method was not affected by fault resistance or phase angle at the instant of the fault. In addition, a transient signal measured over one period was adequate for processing and successfully finding fault distance.

Acknowledgment

This work was supported by the Scientific and Technological Research Council of Turkey (TÜBİTAK) under grant EEEAG-114E152.

References

[1] Grunbaum R, Samuelsson J. Series capacitors facilitate long distance AC power transmission. In: Russia Power Tech; 27–30 June 2005; St. Petersburg, Russia. New York, NY, USA: IEEE. pp. 1-6.

[2] Damnjanovic A, Dayton D, Ferguson G. Assessment modeling of series capacitors protected by metal oxide varistors in power system studies. In: Power Engineering Society General Meeting; 24–28 June 2007; Tampa, FL, USA. New York, NY, USA: IEEE. pp. 1-5.

[3] Vyas B, Maheshwari RP, Das B. Protection of series compensated transmission line: issues and state of art. Electr Pow Syst Res 2014; 107: 93-108.

[4] Al-Dabbagh M, Kapuduwage SK. Using instantaneous values for estimating fault locations on series compensated transmission lines. Electr Pow Syst Res 2005; 76: 25-32.

[5] Malathi V, Marimuthu NS, Baskar S, Ramar K. Application of extreme learning machine for series compensated transmission line protection. Eng Appl Artif Intel 2011; 24: 880-887.

[6] Yusuff AA, Fei C, Jimoh AA, Munda JL. Fault location in a series compensated transmission line based on wavelet packet decomposition and support vector regression. Electr Pow Syst Res 2011; 81: 1258-1265.

[7] Joshi HM, Kothari NH. A review on series compensation of transmission lines and its impact on performance of transmission lines. Int J Eng Dev Res 2014; 72-76.

[8] Sybille G, Le-Huy H. Digital simulation of power systems and power electronics using the MATLAB/Simulink Power System Blockset. In: Power Engineering Society Winter Meeting; 23–27 January 2000; Singapore. New York, NY, USA: IEEE. pp. 2973-2981.

[9] Saha MM, Izykowski J, Rosolowski E, Kasztenny B. A new accurate fault locating algorithm for series compensated lines. IEEE T Power Deliver 1999; 14: 789-797.

[10] Çapar A, Arsoy AB. A performance oriented impedance based fault location algorithm for series compensated transmission lines. Int J Elec Power 2015; 71: 209-214.

[11] Sadeh J, Adinehzadeh A. Accurate fault location algorithm for transmission line in the presence of series connected FACTS devices. Int J Elec Power 2010; 32: 323-328.

[12] Nobakhti SM, Akhbari M. A new algorithm for fault location in series compensated transmission lines with TCSC. Int J Elec Power 2014; 57: 79-89.

[13] Huang Z, Chen Y, Gong Q. A protection and fault location scheme for EHV line with series capacitor based on travelling waves and wavelet analysis. In: International Conference on Power System Technology; 13–17 October 2002; Kunming, China. pp. 290-294.

[14] Abedini M, Hasani A, Hajbabaie AH, Khaligh V. A new traveling wave fault location algorithm in series compensated transmission line. In: 21st Iranian Conference on Electrical Engineering; 14–16 May 2013; Mashhad, Iran. pp. 1-6.

[15] Mamiş MS, Arkan M. FFT based fault location algorithm for transmission lines. In: 7th International Conference on Electrical and Electronics Engineering; 1–4 December 2011; Bursa, Turkey. pp. 71-75.

[16] Mamiş MS, Arkan M, Keleş C. Transmission lines fault location using transient signal spectrum. Int J Elec Power 2013; 53: 714-718.

[17] Akmaz D, Mamiş MS, Arkan M, Tağluk ME. Fault location on series compensated power transmission lines using transient spectrum. In: 23rd Signal Processing and Communications Applications Conference; 16–19 May 2015; Malatya, Turkey. pp. 951-954.

[18] Akmaz D, Mamiş MS, Arkan M, Tağluk ME. Travelling-wave based fault distance estimation for series compensated transmission lines using EMTP-ATP. In: EEUG European EMTP-ATP Conference; 14–18 Sept. 2015; Grenoble, France. pp. 151-161.

[19] Meyer WS. Liu T. Alternative Transient Program (ATP) Rule Book. Portland, OR, USA: Canadian-American EMTP User Group, 1992.

[20] Stevenson WD. Elements of Power System Analysis. 4th ed. New York, NY, USA: McGraw-Hill, 1982.

[21] Marti JR. Accurate modeling of frequency-dependent transmission-lines in electromagnetic transient simulations. IEEE T Power Ap Syst 1982; 101: 147-157.

[22] Abur A, Ozgun O, Magnago FH. Accurate modeling and simulation of transmission line transients using frequency dependent modal transformations. In: Power Engineering Society Winter Meeting; 28 January–1 February 2001; Columbus, OH, USA. New York, NY, USA: IEEE. pp. 1443-1448.